Published December 1, 1986

Evidence for Splicing New Basement Membrane into Old during Glomerular Development in Newborn Rat Kidneys

Dale R. Abrahamson and Elizabeth W. Perry

Department of Cell Biology and Anatomy, University of Alabama at Birmingham, Birmingham, Alabama 35294

Abstract. Tannic acid in glutaraldehyde fixatives greatly enhanced the visualization of two developmentally and morphologically distinct stages in glomerular basement membrane (GBM) formation in newborn rat kidneys. First, in early stage glomeruli, double basement membranes between endothelial cells and podocytes were present and, in certain areas, appeared to be fusing. Second, in maturing stage glomeruli, elaborate loops and outpockets of basement membrane projected into epithelial, but not endothelial, sides of capillary walls. When Lowicryl thin sections from newborn rat kidneys were sequentially labeled with rabbit anti-laminin IgG and anti-rabbit IgG-colloidal gold, gold bound across the full width of all GBMs, including double basement membranes and outpockets. The same distribution was obtained when sections from rats that received intravenous injections of rabbit anti-laminin IgG 1 h before fixation were labeled directly with anti-rabbit IgG-colloidal gold. When kidneys were fixed 4 d after anti-laminin IgG injection, however, loops beneath the podocytes in maturing glomeruli were usually unlabeled and lengths of unlabeled GBM were interspersed with labeled lengths. In additional experiments, rabbit anti-laminin IgG was intravenously injected into newborn rats and, 4–14 d later, rats were re-injected with sheep anti-laminin IgG. Sections were then doubly labeled with anti-rabbit and anti-sheep IgG coupled to 10 and 5 nm colloidal gold, respectively. Sheep IgG occurred alone in outpockets of maturing glomeruli and also in lengths of GBM flanked by lengths containing rabbit IgG. These results indicate that, after fusion of double basement membranes, new segments of GBM appear beneath developing podocytes and are subsequently spliced into existing GBM. This splicing provides the additional GBM necessary for expanding glomerular capillaries.

THE renal glomerular basement membrane (GBM)[1] is approximately twice the thickness of most other basement membranes, measuring ~150 nm in rats (8). One reason for its increased thickness is that the GBM originates during development from the apparent fusion or union of two basement membranes: one beneath the vascular endothelium and one beneath the overlying podocytes or visceral epithelium of Bowman's capsule (14, 24–26, 29). This fusion is probably physiologically significant, since, in addition to creating a thicker matrix, it results in a double layer of anionic sites in the lamina rara interna and externa that is important in establishing a charge barrier to serum proteins (11, 13). The fusion of dual basement membranes generally takes place in glomeruli in early stages of nephrogenesis, however, when capillary diameters are relatively small. With continued development, the endothelium flattens against the GBM and becomes fenestrated. The podocytes form foot processes that interdigitate with processes from adjacent podocytes, attach to the outer surface of the GBM (23), and acquire polyanionic surface coats (17, 23). These events take place as glomerular capillary loop diameters are increasing (7, 9, 15), but the mechanism for the assembly of additional GBM in these expanding capillaries has not been examined in detail.

Previous immunofluorescent labeling studies have shown that laminin (10), type IV collagen, and heparan sulfate proteoglycans (21) are all present within developing GBMs. In earlier immunoelectron microscopy experiments, we intravenously injected anti-laminin IgG coupled directly to horseradish peroxidase (HRP) into newborn rats (2). This labeled basement membranes of glomeruli in all stages of development, from embryonic in the outer renal cortex to almost mature in the inner cortex. In addition, we identified, in maturing stage glomeruli in the inner cortex, extensive loops of apparently newly synthesized basement membrane material located between and beneath developing foot processes of podocytes. These loops were not induced in immature rats by the intravenous injection of anti-laminin IgG because identical structures were also identified within glomeruli of normal, uninjected newborns. These loops are normally not seen in adult glomeruli, however. In the studies presented here, we have used techniques for labeling developing GBM in vivo for postembedding immunogold elec-

1. *Abbreviations used in this paper*: GBM, glomerular basement membrane; HRP, horseradish peroxidase.

Published December 1, 1986

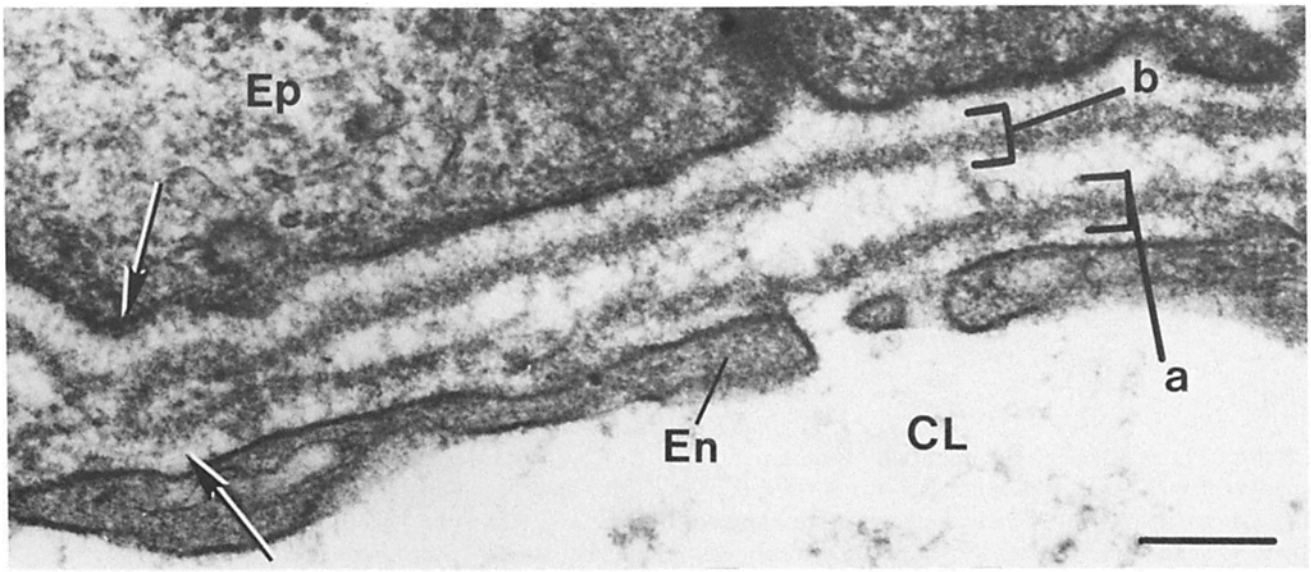

Figure 1. Electron micrograph of early developing capillary loop stage glomerulus from a newborn rat kidney fixed with 1% tannic acid in glutaraldehyde. A double basement membrane ([*a*] and [*b*]) between the endothelium (*En*) and epithelium (*Ep*) is clearly visible. The two basement membranes are closely apposed on the left of the figure (*arrows*) and may be in the process of fusing. *CL*, capillary lumen. Bar, 0.2 μm.

tron microscopy. Our results indicate that the loops of basement membrane seen beneath the epithelium in maturing glomeruli of newborn rat kidneys are spliced into existing GBM as glomerular capillaries undergo expansion.

Materials and Methods

Proteins and Reagents

Laminin was purified from the murine Englebreth-Holm-Swarm sarcoma by salt extraction, ion exchange, and gel filtration chromatography (1, 27), and characterized as previously described (1). Rabbit and sheep anti-laminin IgGs were purified from sera collected from immunized animals, affinity-isolated from columns of laminin-Sepharose, and shown to be highly specific for laminin (1–3). Laminin-adsorbed rabbit and sheep IgGs and commercially prepared IgGs (Cooper Biomedical, Inc., Malvern, PA) were used in control experiments. Anti-laminin and control IgGs were conjugated directly to activated HRP (type VI, Sigma Chemical Co., St. Louis, MO) (22) as before (1–3). Goat anti-rabbit IgG coupled to 10-nm diameter colloidal gold was obtained from Janssen Pharmaceutica (Beerse, Belgium). Rabbit anti-sheep IgG coupled to 5 nm colloidal gold was purchased from E. Y. Laboratories, Inc., San Mateo, CA.

Experimental Procedures

Newborn Sprague-Dawley rats (Southern Animal Farms, Prattville, AL) were anesthetized with ether 2 d after birth. They then received intravenous injections of 0.3 ml of affinity-purified rabbit anti-laminin IgG, rabbit anti-laminin IgG-HRP, or control IgGs (1.0 mg IgG/ml) via the saphenous vein. For double labeling experiments, rats were re-anesthetized 4–14 d later, and these animals then received intravenous injections of 0.4–0.5 ml affinity-purified sheep anti-laminin IgG.

Tissue Processing

The left kidneys from anesthetized rats were clamped at the hilus and the appropriate fixative solution was simultaneously injected into the cortices. Kidney tissues from newborns that had not received IgG injections were fixed in 1% glutaraldehyde and 1% tannic acid in 0.1 M phosphate buffer, pH 7.3, for 2 h, postfixed in 2% osmium in 0.1 M phosphate buffer for 2 h, routinely dehydrated in ethanol, and embedded in epoxy resin (Embed 812; Electron Microscopy Sciences, Fort Washington, PA). For postembedding colloidal gold immunolabeling, cubes of kidney cortex from uninjected rats and those that received anti-laminin IgG or control IgG, were fixed for 2 h in 4% formaldehyde (freshly prepared from paraformaldehyde) in 0.1 M phosphate buffer, pH 7.3. Postfixation with osmium was omitted to preserve immunoreactivity. Tissue was dehydrated in dimethylformamide and embedded at 4°C in Lowicryl K4M medium (Polysciences, Inc., Warrington, PA) using methods described previously (6) with modifications (4). Kidneys from rats injected with IgG-HRP conjugates were fixed, processed for peroxidase histochemistry (12), and routinely dehydrated and embedded as before (1–3).

Postembedding Immunolabeling with Colloidal Gold

All solutions for postembedding immunolabeling, except colloidal gold-IgGs, were filtered through a 0.22-μm cellulose acetate membrane (Corning Glass Works, Corning, NY) before use. The colloidal gold-IgGs were centrifuged for 5 min at 7000 *g* to remove large aggregates. Analysis of Formvar-coated grids of the colloidal gold-IgGs showed that ~80% of the gold particles occurred as singlets (4). Lowicryl sections, 70-nm thick, were picked up on uncoated 400-mesh nickel grids, treated for 1 h with 0.5 M ammonium chloride to inactivate residual aldehydes, and treated for an additional 1 h with 0.1% BSA in PBS to minimize nonspecific labeling. Sections from each of two uninjected rats were then incubated sequentially in drops of 15 μg/ml affinity-purified rabbit anti-laminin IgG, or control IgG, and colloidal gold-anti-rabbit IgG using protocols described previously (4). Lowicryl sections from six rats that received intravenous injections of rabbit anti-laminin IgG, or control IgG (two rats), were incubated directly with anti-rabbit IgG-colloidal gold for 64 h at 4°C in sealed microfuge tubes. Incubations for shorter periods generally resulted in significantly less immunogold labeling with this technique. Sections from five rats that received dual injections of rabbit and sheep anti-laminin IgG, or control IgGs (one rat), were labeled first with anti-rabbit IgG-colloidal gold (10 nm) for 64 h, washed in buffered BSA, and then treated for 24 h with 0.5% normal rabbit serum in buffered albumin. Grids were then re-labeled with anti-sheep IgG-colloidal gold (5 nm) for 64 h. All grids labeled with immunogold were thoroughly washed with buffered albumin and finally with distilled H_2O. Lowicryl sections were then stained for 30 s with 2% uranyl acetate and for 1 min with lead citrate. Electron microscopy was conducted with an accelerating voltage of 60 kV. Lengths of GBM from photographic prints were measured on a digitizing tablet using a computer morphometric program (R & M Biometrics, Inc., Nashville, TN) (2). Gold particle counts were expressed as number of colloidal gold particles per micrometer linear length of GBM.

Results

The two developmentally and morphologically distinct stages of GBM assembly were clearly observed with the ad-

Published December 1, 1986

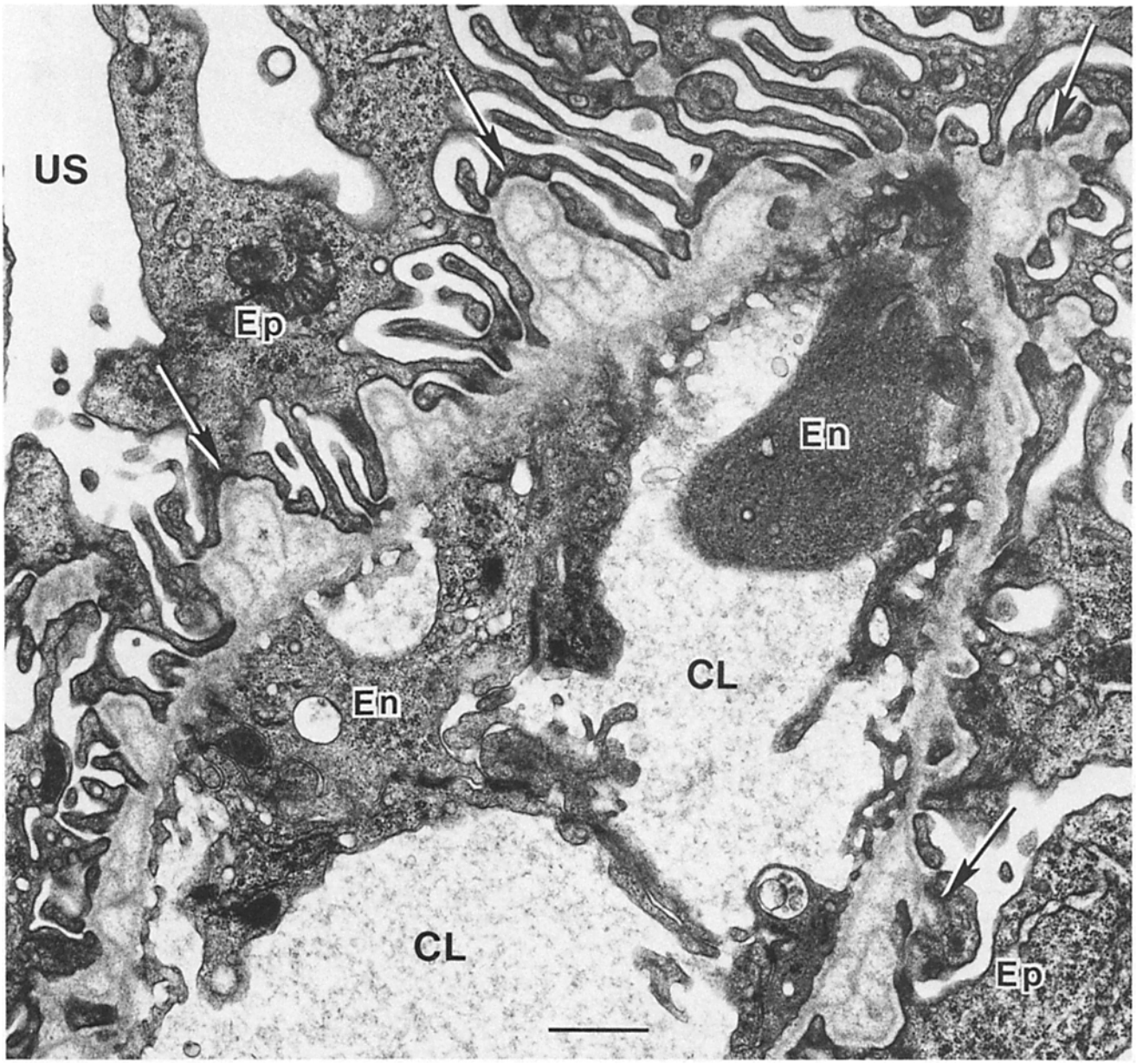

Figure 2. Capillary loop from maturing stage glomerulus of normal newborn rat kidney. Numerous irregular loops and outpockets of basement membrane (*arrows*) are present beneath differentiating foot processes of podocytes (*Ep*). Note that electron-dense and electron-lucent layers within these outpockets can be distinguished. Outpockets do not extend into the endothelial cell layer (*En*). In contrast to outpockets, double basement membranes are generally not observed in maturing stage glomeruli. *CL*, capillary lumen; *US*, urinary space. Bar, 1.0 μm.

dition of tannic acid to aldehyde fixatives (Figs. 1 and 2). First, in early (S-shaped and developing capillary loop stage) glomeruli, the two laminae densae of double basement membranes between developing endothelial cells and podocytes were readily identified (Fig. 1). In some cases, the dual laminae densae were only narrowly separated and in these areas may have been in the process of fusing (Fig. 1). In later, maturing stage glomeruli, elaborate, irregular outpockets and loops of basement membrane projecting into the epithelial sides of capillary walls were often present (Fig. 2). These loops contained electron-dense and electron-lucent layers, probably corresponding to the lamina densa and lamina rara, and were otherwise ultrastructurally identical to mature GBM. Basement membrane outpockets were seen most frequently between and beneath podocyte foot processes undergoing development and interdigitation (Fig. 2). Double basement membranes were rarely seen in glomeruli in these stages.

Postfixation, Postembedding Colloidal Gold Immunolabeling of Laminin

When Lowicryl thin sections of formaldehyde-fixed newborn rat kidneys were sequentially labeled with rabbit anti-laminin IgG and anti-rabbit IgG-colloidal gold, gold particles bound to sections specifically overlying basement membranes (Fig. 3, *a–c*). In developing glomeruli at early stages, gold bound to both laminae densae of double basement membranes as well as to the lamina rara interna beneath the endothelium and the lamina rara externa beneath the epithelium (Fig. 3 *a*). There was little or no gold binding to the

Published December 1, 1986

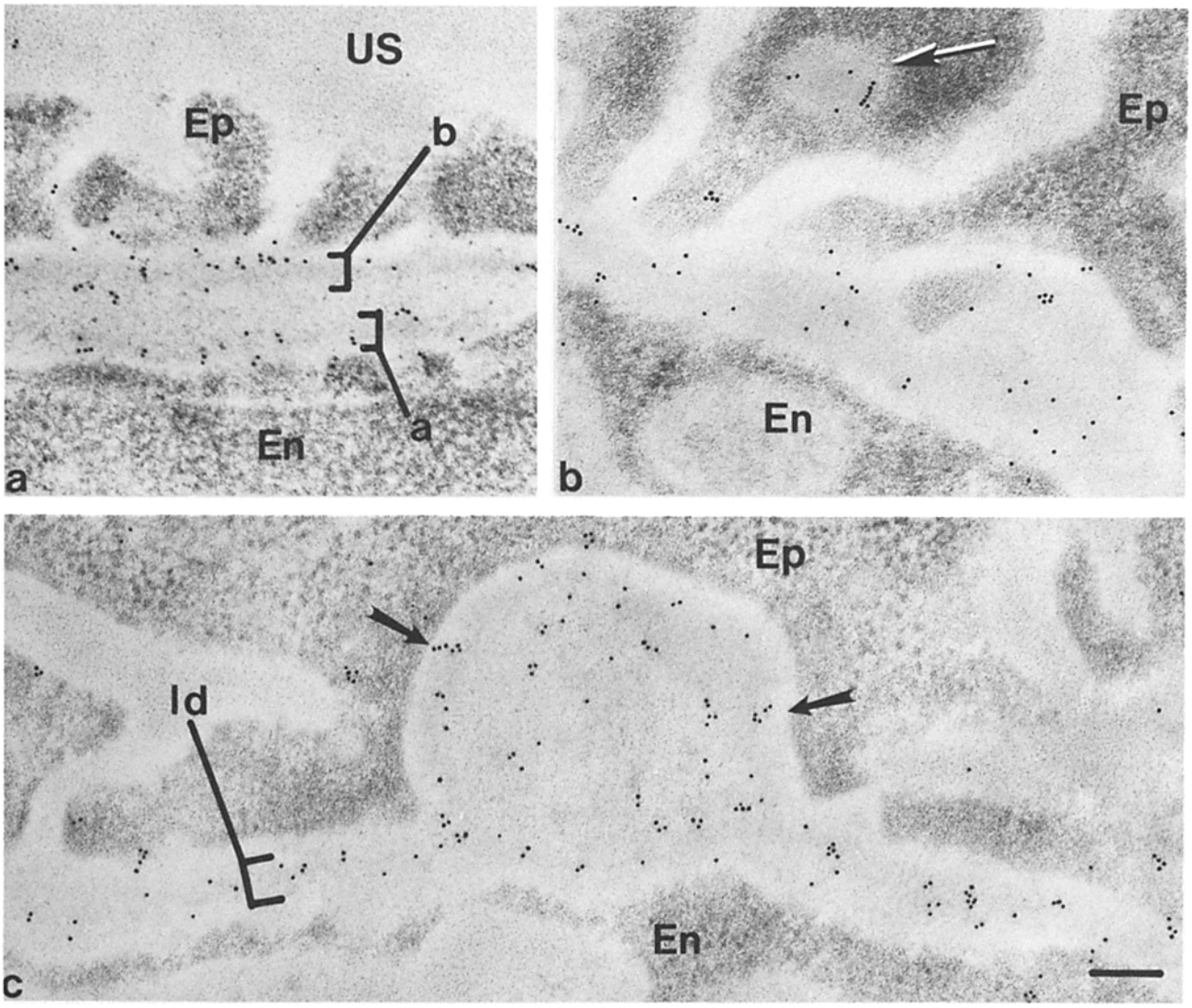

Figure 3. Lowicryl sections of newborn rat kidney glomerular capillary walls from early capillary loop (*a*) and maturing stage (*b* and *c*) glomeruli labeled sequentially with rabbit anti-laminin IgG and anti-rabbit IgG-colloidal gold. (*a*) Both layers ([*a*] and [*b*]) of double basement membranes are labeled with anti-laminin IgG. (*b*) In addition to the GBM of maturing glomeruli, anti-laminin IgG binds to intracellular vesicles within podocytes (*arrow*). (*c*) Anti-laminin IgG is present across the full width of the GBM, binding in large amounts to the lamina densa (*ld*). Antilaminin is also present throughout the full extent of the basement membrane outpocket beneath the epithelium (*arrows*). *En*, endothelium; *Ep*, epithelium; *US*, urinary space. Bar, 0.15 μm.

central region between the two basement membranes when the two laminae densae were widely separated, however (Fig. 3 *a*). In glomeruli at later developmental stages, the full width of the GBM was labeled (Fig. 3, *b* and *c*). In addition, gold bound to intracellular vesicular structures within the glomerular epithelium (Fig. 3 *b*). The basement membrane outpockets found in maturing glomeruli were labeled with anti-laminin IgG throughout their full dimensions (Fig. 3 *c*). Gold was also present in the lamina rara interna, lamina densa, and lamina rara externa of the GBM, but appeared to occur most frequently in the lamina densa (Fig. 3 *c*). Anti-rabbit IgG-colloidal gold did not bind to Lowicryl sections treated with control, laminin-adsorbed rabbit IgG (Fig. 4).

In Vivo Labeling of Laminin Detected by Postembedding Colloidal Gold Techniques

To determine the GBM distribution of anti-laminin IgG introduced in vivo, Lowicryl sections from newborn rats that had received intravenous injections of rabbit anti-laminin IgG 1 h before fixation were treated directly with anti-rabbit IgG-colloidal gold. As shown in Fig. 5 *a*, gold bound exclusively and in high densities to the developing GBM. Intravenously injected anti-laminin IgG was also present throughout the full extent of the basement membrane outpockets characteristic of maturing glomeruli (Fig. 5 *a*) as seen previously when anti-laminin IgG was applied to fixed tissue (Fig. 3 *c*). To evaluate whether the distribution of GBM-bound anti-laminin IgG changed during GBM assembly, rat kidneys were fixed and processed for postembedding immunolabeling 4, 5, and 14 d after IgG injection. Capillary loops in maturing stage glomeruli were then photographed and the numbers of colloidal gold particles bound to the GBM were counted and compared with what was seen 1 h after injection. In general, a marked reduction in colloidal gold binding to Lowicryl sections was seen at 4 d and, in particular, the

Published December 1, 1986

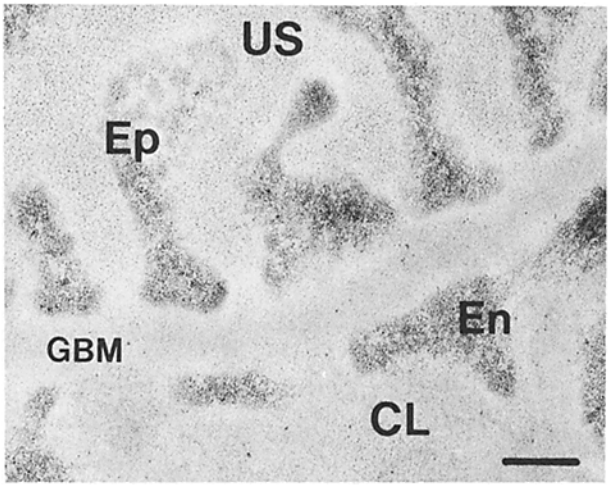

Figure 4. Lowicryl section sequentially treated with control, laminin-adsorbed rabbit IgG and anti-rabbit IgG-colloidal gold. Gold does not bind to the GBM or elsewhere on the section. *CL*, capillary lumen; *En*, endothelium; *Ep*, epithelium; *US*, urinary space. Bar, 0.2 μm.

GBM outpockets were often completely unlabeled (Fig. 5 *b*). Even less gold bound to sections from kidneys fixed 14 d after anti-laminin IgG injection (Fig. 5 *c*). However, gold generally was not restricted to any one layer of the GBM and instead was grouped in small clusters across the full width. In addition, there were unlabeled lengths of GBM interspersed between labeled lengths (Fig. 5 *c*). Anti-rabbit IgG-colloidal gold did not bind to Lowicryl sections from control, uninjected rats, or rats that received injections of laminin-adsorbed rabbit IgG or commercial rabbit IgG.

Anti-Laminin IgG-HRP Experiments

Rats that had received intravenous injections of sheep anti-laminin IgG coupled directly to HRP 1 h before fixation had peroxidase reaction product throughout all of their GBMs, as well as in the outpockets, in apparently uniform densities, as shown before (2). When kidneys were fixed 4–6 d after anti-laminin IgG-HRP injection, however, GBMs in maturing stage glomeruli usually showed highly variable HRP reaction product (Fig. 6). Here, HRP labeling within capillary loops was often interrupted with weakly labeled and unlabeled lengths of GBM (Fig. 6). When present, however, HRP reaction product appeared to extend across the full thickness of GBM except in areas underlying outpockets. In these cases, the outpockets were usually unlabeled with anti-laminin IgG, as previously shown with immunoperoxidase (2), and here with postembedding immunogold labeling techniques (Fig. 5 *b*).

Double Labeling Experiments

Lowicryl sections from rats that had received intravenous injections of rabbit anti-laminin IgG and sheep anti-laminin IgG at separate times of development were doubly labeled with anti-rabbit IgG and anti-sheep IgG coupled to 10 nm and 5 nm diameter colloidal gold, respectively. In these cases, the total amount of either colloidal gold binding to sections was the same as when sections were labeled singly (data reviewed but not shown). In doubly labeled sections from dually injected rats, the distribution patterns of rabbit and sheep anti-laminin IgG in maturing stage glomeruli were frequently different, however. In rats that received sheep anti-laminin IgG 4–14 d after rabbit anti-laminin IgG, sheep, but not rabbit IgG, was often present within GBM outpockets, whereas both IgGs were present together in GBM immediately beneath the outpockets (Fig. 7, *a* and *b*). In addition, in areas of apparently completely assembled GBM, sheep anti-laminin IgG was also present alone in lengths that were flanked by lengths containing rabbit anti-laminin IgG (Fig. 7 *c*).

Discussion

The purpose of these experiments was to further study the process of GBM assembly in developing kidneys. Our observations indicate that in maturing stage glomeruli, newly synthesized matrix, which is probably derived mainly from the podocytes, is spliced into existing GBM.

Laminin Distribution within Developing GBMs

The results from this study with immunogold labeling confirmed earlier experiments with immunoperoxidase (2), showing that anti-laminin IgG bound to the full thickness of each of the double basement membranes found in early stage glomeruli. Since this double basement membrane subsequently appears to fuse, the mature GBM therefore probably contains at least a double layer of laminin. That both the endothelium and epithelium contribute to GBM formation has been previously shown in other studies using anti-type IV collagen antibodies (25). In later developmental stages, however, double basement membranes were generally not present and anti-laminin IgG bound throughout the full width of the GBM between the endothelium and epithelium. Postembedding colloidal gold immunolabeling of laminin in adult kidneys has similarly shown laminin throughout the full width of the mature GBM (4). In addition, laminin was immunolocalized in newborn kidneys throughout the full extent of the irregular loops of basement membrane material that projected into the epithelium of maturing stage glomeruli. Since these loops and outpockets ultrastructurally resemble basement membranes, contain electron-dense and electron-lucent layers corresponding to the lamina densa and lamina rara, and contain anionic sites in the electron-lucent layers as shown by labeling with cationized ferritin (5), we believe that they probably represent at least a precursor form of genuine GBM. Previous experiments suggested that these basement membrane loops were synthesized mainly by the epithelium (2). The immunogold labeling of laminin intracellularly within maturing podocytes, but not the endothelium in maturing glomeruli, therefore supports these earlier observations.

Postembedding Localization of Intravenously Injected Anti-Laminin IgG

Techniques were developed here for labeling developing basement membranes in vivo with the intravenous injection of anti-laminin IgG, and then detecting this GBM-bound IgG with postembedding colloidal gold immunolabeling procedures. In kidneys from animals that had received injections 1 h before fixation, gold was abundantly present throughout the full width of GBM as well as in the outpockets, as seen

Published December 1, 1986

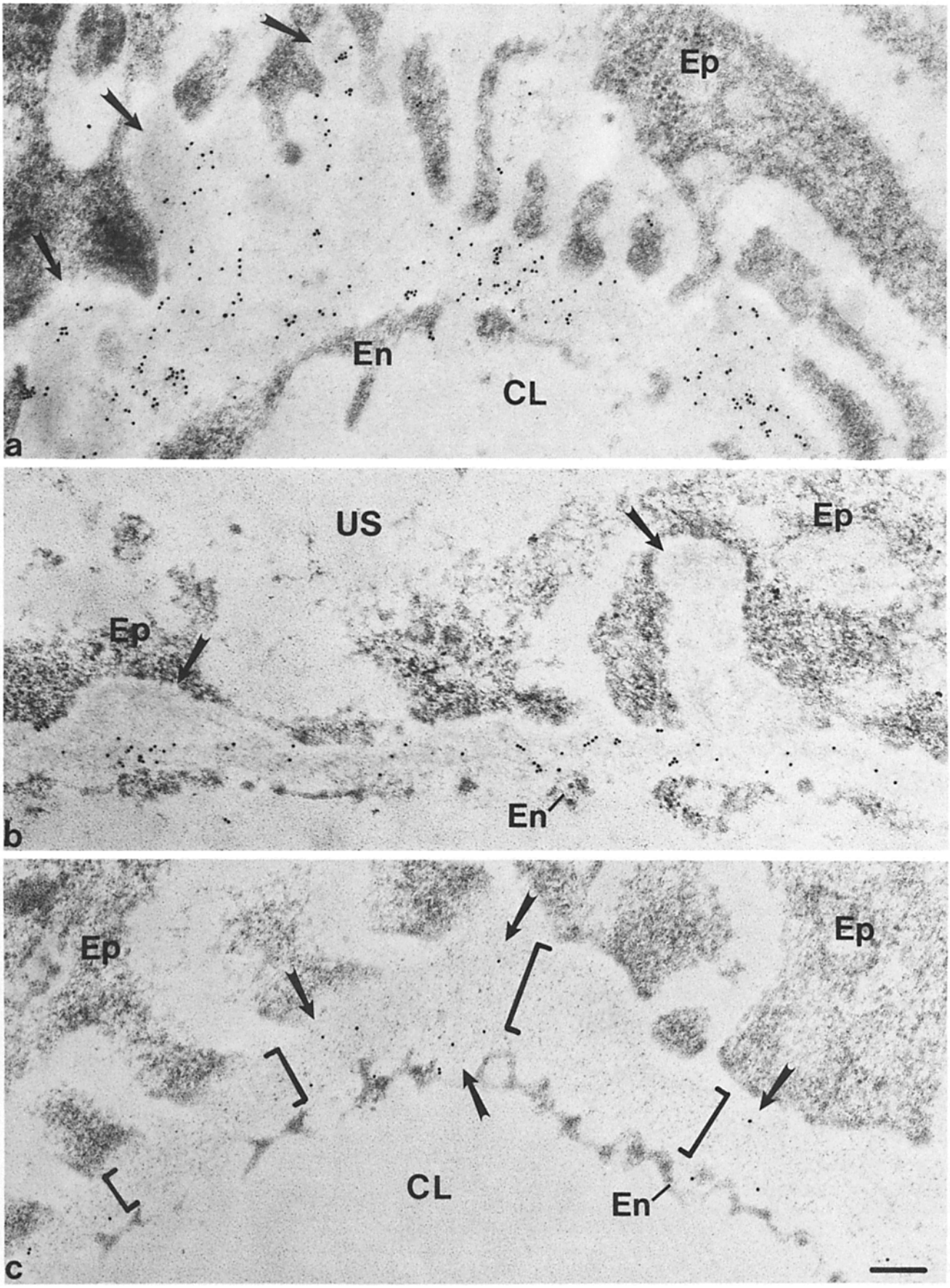

Published December 1, 1986

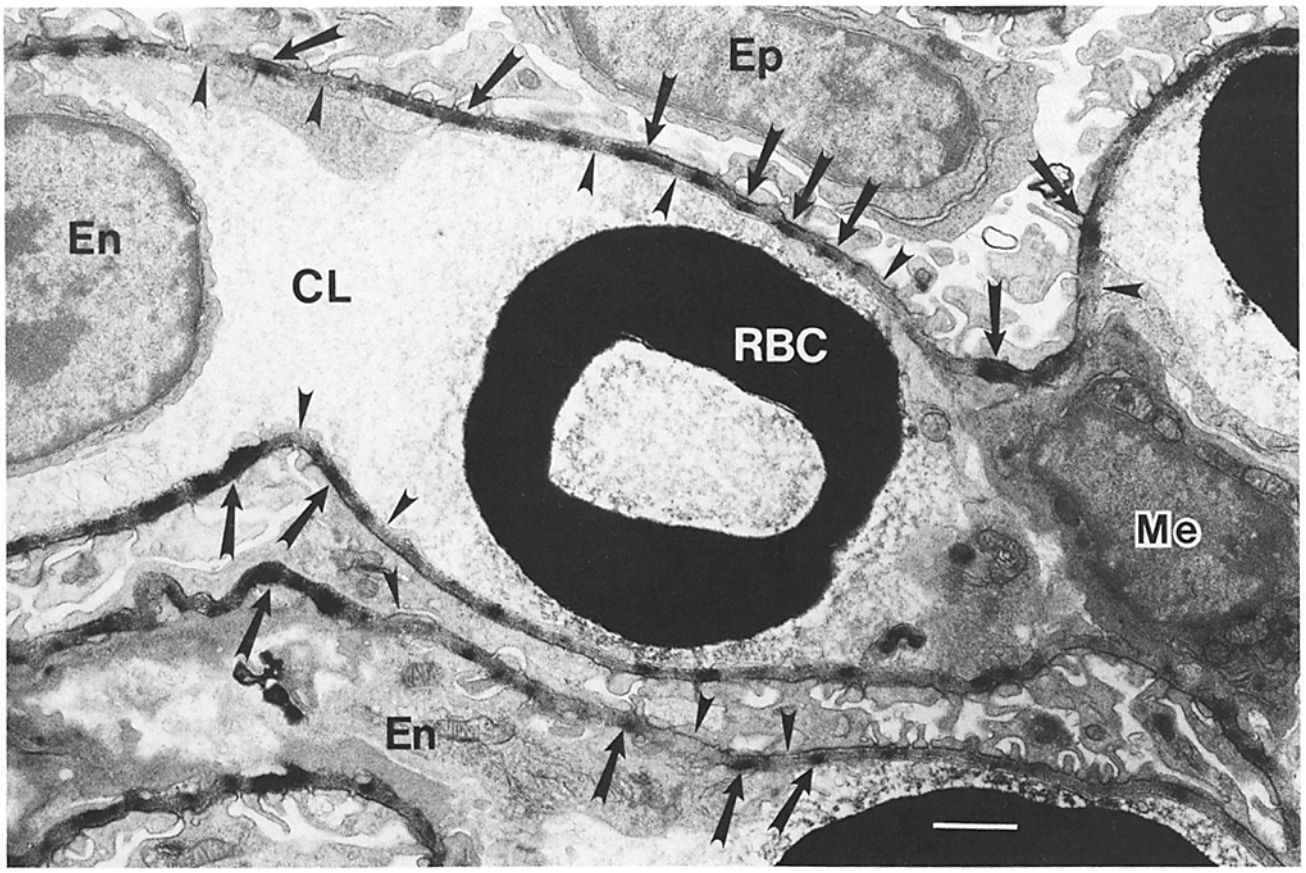

Figure 6. Micrograph of maturing stage glomerulus from a newborn rat that received anti-laminin IgG conjugated directly to HRP 4 d before fixation. When present, HRP reaction product extends across the full thickness of the GBM (*arrows*). The reaction product is nonlinear, however, and is frequently interrupted with unlabeled lengths of GBM (*arrowheads*). *CL*, capillary lumen; *RBC*, erythrocyte; *En*, endothelium; *Me*, mesangial cell; *Ep*, epithelium. Bar, 1.0 μm.

when thin sections from uninjected rats were sequentially processed for routine postembedding immunolabeling. In other words, anti-laminin IgG, whether applied in vivo under presumably normal filtration conditions, or in vitro to fixed, embedded kidney sections, bound in precisely the same distribution patterns to the GBM. When Lowicryl sections from rats that had received injected anti-laminin IgG 4 d previously were labeled, however, significantly less gold bound to the GBM. In addition, the GBM outpockets at this time were usually entirely unlabeled with colloidal gold. This result indicates (*a*) that the unlabeled outpockets were assembled after IgG injection, and (*b*) that anti-laminin IgG, once bound to the GBM in vivo, did not redistribute in discernable amounts to newly synthesized laminin. However, even less anti-rabbit-colloidal gold bound to Lowicryl sections from rats that had received rabbit anti-laminin IgG 14 d before fixation. We do not believe that this progressive reduction in immunogold binding was due to significant levels of in vivo dissociation of anti-laminin IgG from the GBM, however, for several reasons. First, all of the antibodies used in this study were affinity-isolated and, consequently, had been selected for their ability to combine relatively tightly with laminin. Second, quantitative immunofluorescence microscopy of mature rat glomeruli labeled in vivo with anti-laminin IgG has previously shown that most of the bound IgG remains stably associated with the GBM for at least several weeks (3). Immunofluorescence microscopy of newborn rat kidneys has also shown persistent binding of anti-laminin IgG to developing GBM (2). Finally, when kidneys labeled in vivo with anti-laminin IgG–HRP 4–6 d before fixation were examined, HRP reaction product in capillary loop GBM of maturing stage glomeruli was, in areas, nonlinear and was punctuated with numerous unlabeled sections of GBM. The possibility that anti-laminin IgG–HRP completely dissociated from some lengths of GBM, but not others, therefore seems unlikely. Nevertheless, patterns of

Figure 5. Lowicryl sections from newborn rats that received intravenous injections of rabbit anti-laminin IgG 1 h (*a*), 4 (*b*), and 14 d (*c*) before fixation. Unlike Fig. 3, *a–c*, these sections were treated only with anti-rabbit IgG-colloidal gold. (*a*) 1 h after anti-laminin IgG injection, gold binds to rabbit IgG exposed on the surface of the section specifically over the GBM as well as on the loops and outpockets (*arrows*) beneath developing foot processes of the epithelium (*Ep*). This distribution of gold across the full width of the GBM is similar to what is seen with sequential labeling of kidney sections from uninjected rats (Fig. 3, *a–c*). (*b*) 4 d after injection, less gold is present over the GBM, and outpockets beneath the epithelium (*Ep*) are unlabeled (*arrows*). (*c*) 14 d after injection, even less gold binds to the GBM and stretches of unlabeled GBM (*brackets*) are present between labeled lengths (*arrows*). *CL*, capillary lumen; *En*, endothelium; *US*, urinary space. Bar, 0.2 μm.

Published December 1, 1986

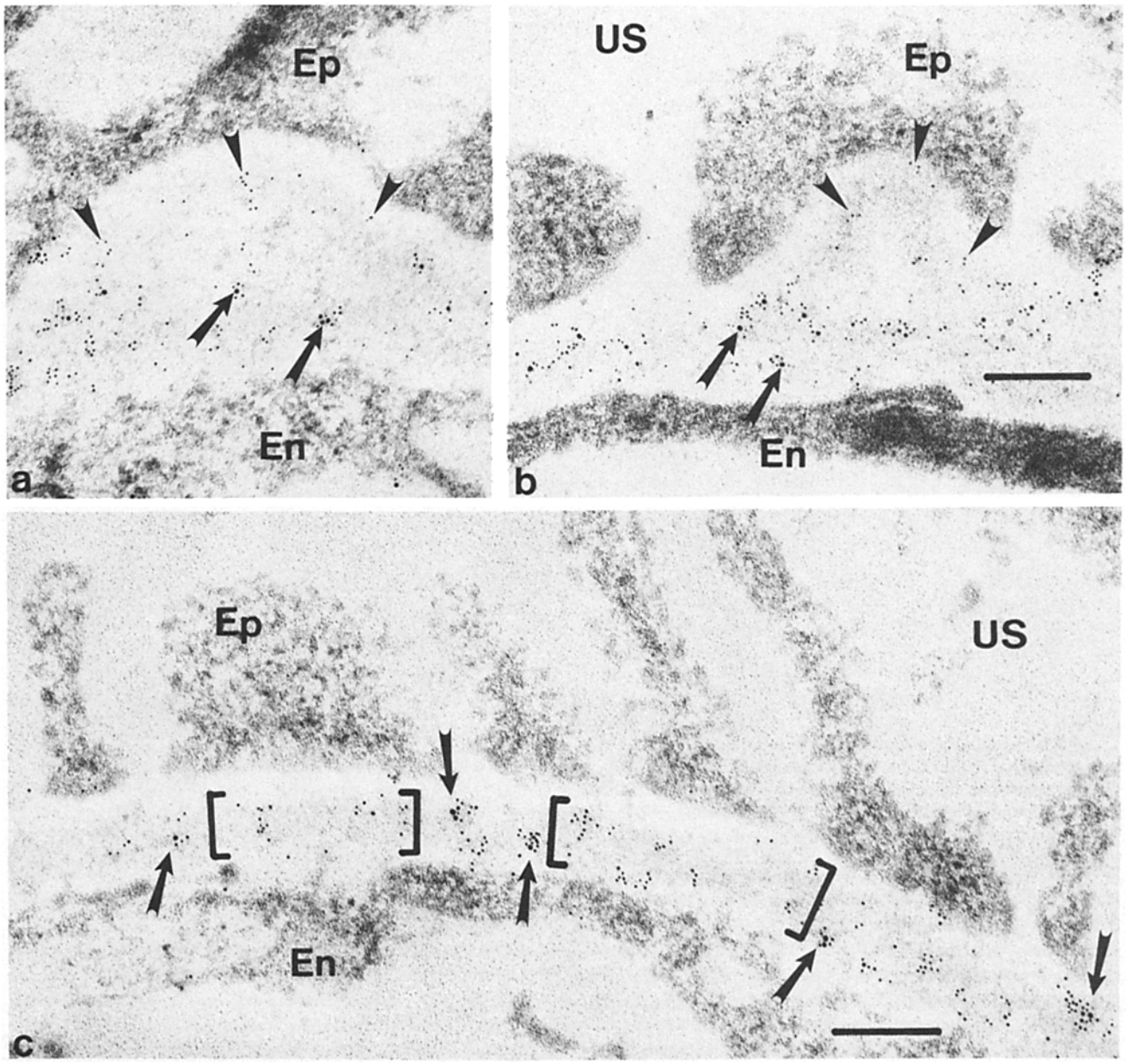

Figure 7. Lowicryl sections from rats that received rabbit anti-laminin IgG at 2 d of age and were then re-injected with sheep anti-laminin IgG at 6 (*a* and *b*) or 16 d of age (*c*). Kidneys were fixed 1 h after sheep IgG injection. Sections were doubly labeled with anti-rabbit IgG–10 nm colloidal gold and anti-sheep IgG–5 nm colloidal gold. In *a* and *b*, only sheep anti-laminin IgG is present within the outpockets (*arrowheads*) whereas both sheep and rabbit IgG (*arrows*) are present together in subjacent GBM. In *c*, there are lengths of GBM that contain only sheep IgG (*brackets*) interspersed with segments containing rabbit IgG (*arrows*). (cf. Fig. 5 *c*). *En*, endothelium; *Ep*, epithelium; *US*, urinary space. Bars, 0.2 μm.

bound IgG clearly changed quantitatively with subsequent development. As discussed below, we believe that this primarily reflects the addition of newly synthesized basement membrane into expanding glomerular walls.

In further experiments, newborn rats that had received rabbit anti-laminin IgG were re-injected 4–14 d later with sheep anti-laminin IgG and the different IgGs were then localized in Lowicryl sections by postembedding double immunolabeling with the appropriate gold conjugates of distinguishable sizes. The results showed that sheep IgG often occurred alone within the GBM outpockets and in lengths of apparently mature GBM that were usually flanked on either side with stretches of GBM containing rabbit IgG. Taken together, we believe that the best interpretation of these findings is that in maturing stage glomeruli, new segments or patches of basement membrane, which first appear by transmission electron microscopy as loops and outpockets beneath the podocytes, are spliced into existing GBM. This process would result in the dilution of old GBM with new, and, therefore, would explain the overall reduction in immunogold binding to sections from newborn rats fixed several days after in vivo GBM labeling. The interrupted pat-

Published December 1, 1986

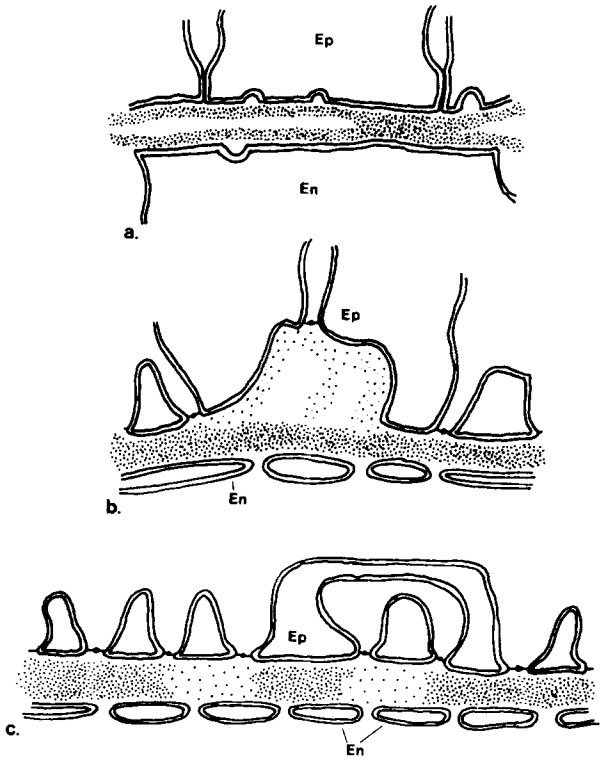

Figure 8. Schematic diagram of the GBM assembly process occurring in glomerular development. (*a*) During early stages of glomerulogenesis, the double basement membranes between the endothelium (*En*) and epithelium (*Ep*) become closely aligned and fuse. (*b*) With continued development, the endothelium (*En*) flattens against the GBM and fenestrations develop. The podocytes (*Ep*) form extensive foot processes, synthesize additional basement membrane material, and loops and outpockets of basement membrane appear beneath developing foot processes in maturing stage glomeruli. (*c*) The newly synthesized GBM from the epithelium joins existing GBM by splicing. Multiple splicing events thereby provide additional GBM for expanding glomerular capillary walls.

terns of HRP reaction product seen in GBMs of rats fixed several days after receiving anti-laminin IgG–HRP could be similarly explained.

Mechanisms of GBM Assembly

Based on our results and those from other laboratories (14, 24, 26, 29), we propose the sequence of events diagramed in Fig. 8 for assembly of the GBM during development. Major features of this model are (*a*) the fusion of endothelial and epithelial basement membranes in early stages of glomerular capillary formation, (*b*) synthesis of additional basement membrane by the epithelium with continued development, and (*c*) joining of the new basement membrane with the GBM by splicing. Although the mechanisms for fusion and splicing are not understood, they are probably mediated, at least in part, by specific binding interactions among the various basement membrane macromolecules (16, 28, 30, 31) that may weave basement membranes together. This mechanism for basement membrane formation is likely to be functionally important, since the filtration of plasma by the GBM is occurring simultaneously with rapid expansion of glomerular capillary walls. Thus, an increase in glomerular filtration surface area can be achieved by the progressive splicing of new patches of basement membrane into existing GBM. Splicing of newly synthesized basement membrane into existing matrix may not be restricted to developing renal glomeruli, however, and may take place frequently in other sites during development as well as during wound healing.

Once the glomerulus has fully blossomed, widespread splicing of new basement membrane patches into the GBM is no longer necessary and extensive basement membrane outpockets beneath the epithelial podocytes are normally not observed in mature kidneys. However, numerous subepithelial knobs or spikes of basement membrane, which are ultrastructurally similar to the outpockets seen here in immature rats, have recently been reported in adult rats and mice with different forms of experimental anti-GBM glomerulonephritis (18–20). In addition, subepithelial knobs are a relatively common structural feature of several human nephropathies. This may be due, among other possibilities, to a resumption of high levels of basement membrane biosynthesis by podocytes in response to injury.

We thank Mrs. Maxine Rudolph for skillfully wordprocessing the manuscript.

These experiments were funded by a grant from the National Institutes of Health (AM-34972). Dr. Abrahamson is an Established Investigator of the American Heart Association.

Received for publication 6 June 1986, and in revised form 8 August 1986.

References

1. Abrahamson, D. R., and J. P. Caulfield. 1982. Proteinuria and structural alterations in rat glomerular basement membranes induced by intravenously injected anti-laminin immunoglobulin G. *J. Exp. Med.* 156:128–145.

2. Abrahamson, D. R. 1985. Origin of the glomerular basement membrane visualized after in vivo labeling of laminin in newborn rat kidneys. *J. Cell Biol.* 100:1988–2000.

3. Abrahamson, D. R., and J. P. Caulfield. 1985. Distribution of laminin within rat and mouse renal, splenic, intestinal, and hepatic basement membranes identified after the intravenous injection of heterologous anti-laminin IgG. *Lab. Invest.* 52:169–181.

4. Abrahamson, D. R. 1986. Post-embedding colloidal gold immunolocalization of laminin to the lamina rara interna, lamina densa, and lamina rara externa of renal glomerular basement membranes. *J. Histochem. Cytochem.* 34: 847–853.

5. Abrahamson, D. R., and E. W. Perry. Distribution of intravenously injected cationized ferritin within developing glomerular basement membranes of newborn rat kidneys. Anat. Rec. In press.

6. Altman, L. G., B. G. Schneider, and D. S. Papermaster. 1984. Rapid embedding of tissues in Lowicryl K4M for immunoelectron microscopy. *J. Histochem. Cytochem.* 32:1217–1223.

7. Aoki, A. 1966. Development of the human renal glomerulus. I. Differentiation of the filtering membrane. *Anat. Rec.* 155:339–352.

8. Caulfield, J. P., and M. G. Farquhar. 1974. The permeability of glomerular capillaries to graded dextrans. Identification of the basement membrane as the primary filtration barrier. *J. Cell Biol.* 63:883–903.

9. DuBois, A. M. 1969. The embryonic kidney. *In* The Kidney: Morphology, Biochemistry, and Physiology. C. Rouiller and A. F. Muller, editors. Vol. 1. Academic Press, Inc., New York. 1–60.

10. Ekblom, P. 1981. Formation of basement membranes in the embryonic kidney: an immunohistological study. *J. Cell Biol.* 91:1–10.

11. Farquhar, M. G. 1981. The glomerular basement membrane: a selective macromolecular filter. *In* Cell Biology of Extracellular Matrix. E. D. Hay, editor. Plenum Publishing Corp., New York. 335–378.

12. Graham, R. C., and M. J. Karnovsky. 1966. The early stages of absorption of injected horseradish peroxidase in the proximal tubules of mouse kidney. Ultrastructural cytochemistry by a new technique. *J. Histochem. Cytochem.* 14:291–302.

13. Kanwar, Y. S. 1984. Biology of disease. Biophysiology of glomerular filtration and proteinuria. *Lab. Invest.* 51:7–21.

14. Kazimierczak, J. 1971. Development of the renal corpuscle and the juxtaglomerular apparatus. A light and electron microscopic study. *Acta. Pathol. Microbiol. Scand.* [A](Suppl.) 218:1–61.

15. Kazimierczak, J. 1980. A study by scanning (SEM) and transmission (TEM) electron microscopy of the glomerular capillaries in developing rat kid-

ney. *Cell Tissue Res.* 212:241–255.

16. Kleinman, H. K., M. L. McGarvey, J. R. Hassell, G. R. Martin, A. B. van Evercooven, and M. Dubois-Dalcq. 1984. The role of laminin in basement membranes and in the growth, adhesion, and differentiation of cells. *In* The Role of Extracellular Matrix in Development. Robert L. Trelstad, editor. Alan R. Liss, Inc. New York. 123–143.

17. Kunz, A., D. Brown, and L. Orci. 1984. Appearance of *Helix pomatia* lectin-binding sites on podocyte plasma membrane during glomerular differentiation. A quantitative analysis using the lectin-gold technique. *Lab. Invest.* 51: 317–324.

18. Makino, H., J. T. Gibbons, M. K. Reddy, and Y. S. Kanwar. 1986. Nephritogenicity of antibodies to proteoglycans of the glomerular basement membrane - I. *J. Clin. Invest.* 77:142–156.

19. Matsuo, S., J. R. Brentjens, G. Andres, J.-M. Foidart, G. R. Martin, and A. Martinez-Hernandez. 1986. Distribution of basement membrane antigens in glomeruli of mice with autoimmune glomerulonephritis. *Am. J. Pathol.* 122:36–49.

20. Miettinen, A., J. L. Stow, S. Mentone, and M. G. Farquhar. 1986. Antibodies to basement membrane proteoglycans bind to the laminae rarae of the glomerular basement membrane (GBM) and induce subepithelial GBM thickening. *J. Exp. Med.* 163:1064–1084.

21. Mounier, F., J.-M. Foidart, and M.-C. Gubler. 1986. Distribution of extracellular matrix glycoproteins during normal development of human kidney. An Immunohistochemical study. *Lab. Invest.* 54:394–401.

22. Nakane, P. K., and A. Kawaoi. 1974. Peroxidase-labeled antibody. A new method of conjugation. *J. Histochem. Cytochem.* 22:1084–1091.

23. Reeves, W., J. P. Caulfield, and M. G. Farquhar. 1978. Differentiation of epithelial foot processes and filtration slits. Sequential appearance of occluding junctions, epithelial polyanion, and slit membranes in developing glomeruli. *Lab. Invest.* 39:90–100.

24. Reeves, W. H., Y. S. Kanwar, and M. G. Farquhar. 1980. Assembly of the glomerular filtration surface. Differentiation of anionic sites in glomerular capillaries of newborn rat kidney. *J. Cell Biol.* 85:735–753.

25. Sariola, H., R. Timpl, K. von der Mark, R. Mayne, J. M. Fitch, T. F. Linsenmayer, and P. Ekblom. 1984. Dual origin of glomerular basement membrane. *Dev. Biol.* 101:86–96.

26. Thorning, D., and R. Vracko. 1977. Renal glomerular basal lamina scaffold. Embryological development, anatomy, and role in cellular reconstruction of rat glomeruli injured by freezing and thawing. *Lab. Invest.* 37:105–119.

27. Timpl, R., H. Rohde, P. G. Robey, S. I. Rennard, J.-M. Foidart, and G. R. Martin. 1979. Laminin—a glycoprotein from basement membranes. *J. Biol. Chem.* 254:9933–9937.

28. Timpl, R., S. Fujiwara, M. Dziadek, M. Aumailley, S. Weber, and J. Engel. 1984. Laminin, proteoglycan, nidogen and collagen IV: structural models and molecular interactions. *Ciba. Found. Symp.* 108:25–43.

29. Vernier, R. L., and A. Birch-Andersen. 1962. Studies of the human fetal kidney. I. Development of the glomerulus. *J. Pediatr.* 60:754–767.

30. Woodley, D. T., C. N. Rao, J. R. Hassell, L. A. Liotta, G. R. Martin, and H. K. Kleinman. 1983. Interactions of basement membrane components. *Biochem. Biophys. Acta.* 761:278–283.

31. Yurchenco, P. D., E. C. Tsilibary, A. S. Charonis, and H. Furthmayr. 1986. Models for the self-assembly of basement membrane. *J. Histochem. Cytochem.* 34:93–102.